

## Bias-stimulated nucleation of silver prepared by pulsed arc deposition on silicon oxide

Andriy Romanyuk, Roland Steiner, Verena Thommen, Peter Oelhafen, and Daniel Mathys

Citation: [Journal of Applied Physics](#) **100**, 074904 (2006); doi: 10.1063/1.2355549

View online: <http://dx.doi.org/10.1063/1.2355549>

View Table of Contents: <http://scitation.aip.org/content/aip/journal/jap/100/7?ver=pdfcov>

Published by the [AIP Publishing](#)

---

### Articles you may be interested in

[Ag films grown by remote plasma enhanced atomic layer deposition on different substrates](#)

J. Vac. Sci. Technol. A **34**, 01A126 (2016); 10.1116/1.4936221

[Optimization of in situ plasma oxidation of metallic gadolinium thin films deposited by high pressure sputtering on silicon](#)

J. Vac. Sci. Technol. B **31**, 01A112 (2013); 10.1116/1.4769893

[Chemically enhanced physical vapor deposition of tantalum nitride-based films for ultra-large-scale integrated devices](#)

J. Vac. Sci. Technol. B **22**, 2734 (2004); 10.1116/1.1808744

[Pulsed bias magnetron sputtering of thin films on insulators](#)

J. Vac. Sci. Technol. A **17**, 3322 (1999); 10.1116/1.582060

[Nitridation of silicon oxide layers by nitrogen plasma generated by low energy electron impact](#)

Appl. Phys. Lett. **71**, 1978 (1997); 10.1063/1.119760

---

**SHIMADZU**  
Excellence in Science

**Powerful, Multi-functional UV-Vis-NIR and FTIR Spectrophotometers**

Providing the utmost in sensitivity, accuracy and resolution for applications in materials characterization and nano research

- Photovoltaics
- Polymers
- Thin films
- Paints
- Ceramics
- DNA film structures
- Coatings
- Packaging materials

[Click here to learn more](#)

Four Shimadzu spectrophotometers are shown. From left to right: a small benchtop model, a larger benchtop model with a sample holder, a large floor-standing model with a sample holder, and a large floor-standing model with a sample holder and a control panel.

# Bias-stimulated nucleation of silver prepared by pulsed arc deposition on silicon oxide

Andriy Romanyuk,<sup>a)</sup> Roland Steiner, Verena Thommen, and Peter Oelhafen  
*Institute of Physics, University of Basel, Klingelbergstrasse 82, 4056 Basel, Switzerland*

Daniel Mathys  
*Microscopy Center, University of Basel, Klingelbergstrasse 50/70, 4056 Basel, Switzerland*

(Received 27 March 2006; accepted 7 July 2006; published online 4 October 2006)

The nucleation and interface formation between Ag films and native silicon oxide have been studied with x-ray and ultraviolet photoelectron spectroscopies. Silver was deposited stepwise onto silicon native oxide by pulsed arc deposition technique onto grounded and biased substrates resulting in kinetic energy of incident silver ions of 95 and 720 eV, respectively. We show that an increase in the kinetic energy of silver ions leads to more homogeneous nucleation and earlier coalescence of Ag films due to surface defect generation and preferential sputtering of oxygen. In addition, deposition from high energy beam results in the formation of an extended transition layer containing a mixture of Ag and Si oxide that might be beneficial in improving adhesion of Ag films. © 2006 American Institute of Physics. [DOI: [10.1063/1.2355549](https://doi.org/10.1063/1.2355549)]

## I. INTRODUCTION

Metal/oxide multilayers are widely used in the production of optical filters and low emissivity coatings for energy saving applications.<sup>1</sup> Silver is the best candidate for the metal component in such multilayer structures due to its high transmittance in the visible range and high reflection in the infrared range. However, the use of silver is restricted by its poor adhesion to insulating substrates, which is a major cause of coating instability and drift. Furthermore, optical performance of the systems with integrated thin silver films is closely related to the dc conductivity of the film, which is strongly thickness related.<sup>2</sup> The effective dc conductivity decreases with decreasing volume concentration of the metal component and vanishes when the concentration approaches the so-called percolation threshold.<sup>3</sup> Near the percolation threshold, silver possesses a large enhancement of optical nonlinearities due to the surface plasmon resonance in the metallic granules and clusters, thus affecting the device performance.<sup>2,4</sup>

The growth of silver on dielectric substrates has already been intensively studied.<sup>5–10</sup> The properties of silver films are strongly dependent on the deposition process and deposition parameters.<sup>11</sup> Commonly used deposition techniques include electron-beam evaporation, laser evaporation, and sputtering. Considerable effort has been made in the investigation of the effect of substrate ion treatment on Ag-film growth kinetics.<sup>12–14</sup> Numerous publications have mainly concentrated on the influence of ion treatment type, ion dose, and ion energy on nucleation kinetics and growth mode [two dimensional (2D) or three dimensional (3D)].

Metal films can also be fabricated using the high energy flux of metal plasma generated by a vacuum arc discharge.<sup>15</sup> The method, often denoted as “cathodic arc plasma deposition (CAPD),” produces dense, highly adherent thin films

and is commonly used in industrial coating applications. The pulsed plasma arc source (PPAS) used in the present study is an adapted CAPD technology which provides precise deposition control allowing us to investigate the early stages of film growth and interface formation.

In the present study we describe the influence of substrate bias on the interface formation between native silicon oxide and silver deposited from the pulsed arc source. The development of the metal/oxide interface is monitored using ultraviolet photoelectron spectroscopy (UPS) and x-ray photoelectron spectroscopy (XPS), which yield information on the chemical composition and electronic structure of the interface components. The size and spatial distributions of Ag islands were measured with scanning electron microscopy (SEM) at early stages of the film growth in order to obtain information about nucleation and subsequent growth mechanisms.

## II. EXPERIMENTAL DETAILS

Boron doped Si(100) wafers (resistivity of 7–21  $\Omega$  cm) covered with a thin (2 nm) native oxide layer were used as substrates for silver deposition. The substrate’s surface roughness measured with atomic force microscopy (AFM) and defined as an arithmetic average of the absolute values of the surface height deviations is found to be  $\sim 0.1$  nm. The wafers were cleaned in acetone and ethanol and introduced into the vacuum system. Prior to metal deposition the substrates were annealed in vacuum at 600 °C for 20 min to remove surface hydroxyls and carbonates.

The pulsed plasma arc source from RHK Technology was used for the silver deposition. The discharge was started by a high voltage pulse (18 kV in our setup) to trigger the electrode. The trigger initiates the main anode-cathode circuit producing a vacuum arc on the target (cathode) surface. During the discharge the silver surface is vaporized and ionized. The created flux of ionized metal plasma consists of Ag

<sup>a)</sup>Electronic mail: andriy.romanyuk@unibas.ch

ions as well as micrometer-sized Ag droplets. These droplets are suppressed by means of a magnetic filter that allows only charged particles to exit the source. The kinetic energy of ions impinging the grounded substrate was estimated to be about 95 eV according to the procedure described in detail by Garnier *et al.*<sup>16</sup> In the second set of experiments the substrate was biased to  $-300$  V, resulting in the kinetic energy of the incident ions at about 720 eV.

*In-situ* photoelectron spectroscopy analysis was performed on a VG ESCALAB 210 spectrometer with a base pressure around  $1 \times 10^{-7}$  Pa during spectra acquisition. Monochromatized Al  $K\alpha$  radiation (1486.6 eV) was used to record the core-level spectra [monochromated x-ray photoelectron spectroscopy (MXPS)] and a helium gas discharge lamp (He I, 21.22 eV) was used to measure the valence band spectra (UPS). The typical resolution was 0.1–0.2 eV for UPS and 0.5 eV for the MXPS measurements. The binding energy scale was calibrated using a clean gold sample and positioning the Au  $4f_{7/2}$  line at 84.0 eV binding energy. In order to obtain integrated core line intensities and peak positions of chemically shifted components, a fit procedure using Doniach-Sunjic functions<sup>17</sup> was applied after a Shirley background subtraction.<sup>18</sup>

The surface morphology of the deposited silver was assessed with SEM at different stages of the film growth process. SEM micrographs were obtained with a Hitachi S-4800.

### III. RESULTS AND DISCUSSION

The valence band spectra (He I) measured as a function of silver deposited onto the native silicon oxide are shown in Fig. 1 for (a) grounded and (b) biased substrates. The bottommost spectrum measured on uncovered silicon oxide is dominated by a broad peak at 8 eV binding energy from the

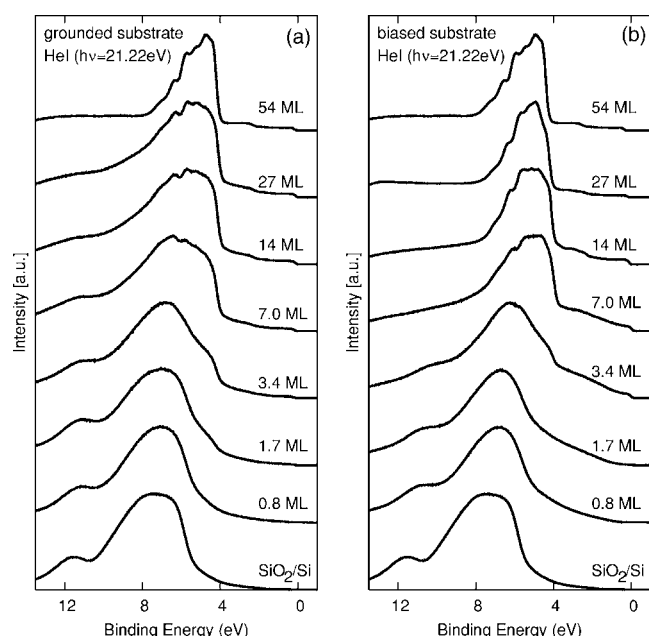


FIG. 1. Evolution of the valence band spectra (He I) as a function of the amount of silver deposited on grounded (left-hand side) and biased (right-hand side) silicon substrate covered with 2 nm native silicon oxide layer.

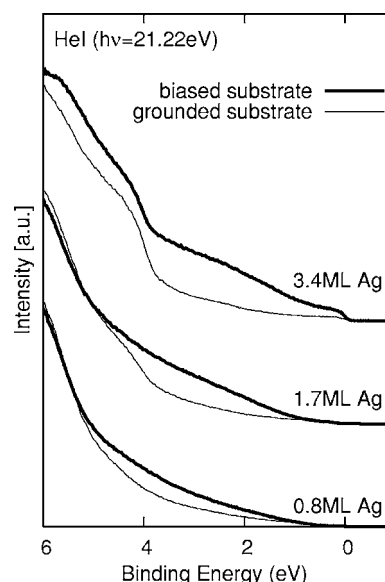


FIG. 2. Valence band spectra (He I) near Fermi cutoff as a function of the amount of silver deposited on grounded (thin lines) and biased (thick lines) silicon substrate covered with 2 nm native silicon oxide layer.

oxygen  $p$  band. Deposition of silver on the grounded substrate [Fig. 1(a)] leads to a broadening of the spectrum and to an intensity increase on the low-binding energy side corresponding to the emission from the silver  $d$  band at 4.7 eV. This trend is continued with increasing silver coverage and the  $d$  band structure becomes more pronounced. The oxygen  $p$  band disappears at silver coverages above 27 ML (monolayer) and for coverage of 54 ML, and the spectrum is identical to the one obtained for thick Ag films.

In contrast to the measurements on a grounded substrate, the evolution of the valence band spectra is different in the case of a biased substrate [Fig. 1(b)]. For silver coverages above 14 ML the valence band spectrum is governed by the emission from the silver  $d$  band and contributions from the oxygen  $p$  band are not visible anymore, implying the formation of a closed metal film. It is interesting to note that the deposition of small amounts of silver leads to a gradual increase of intensity between 1 and 4 eV that might originate from the amorphous silicon  $p$  band. The difference is best shown in Fig. 2, where the valence band spectra measured on grounded and biased substrates for different amounts of silver are superimposed. This increase of intensity may indicate the reduction of silicon oxide by incident Ag ions. In order to deduce additional information on chemical composition of the interface, the core-level spectra are discussed in the following paragraphs.

Figure 3 shows the Si  $2p$  core-level line together with fit results for different Ag amounts deposited on the (a) grounded and (b) biased substrates. The bottommost spectrum corresponds to the silicon oxide on top of the silicon substrate in the absence of the metal deposit. The spectrum consists of three features: one doublet at binding energy of 99.2 eV for the  $2p_{3/2}$  doublet component and spin-orbit splitting energy  $\Delta$  of 0.6 eV that is related to the pure silicon, and two lines located at 100.5 and 103.3 eV corresponding to silicon in the  $\text{Si}^{1+}$  and  $\text{Si}^{4+}$  oxidation states, respectively.<sup>19</sup>

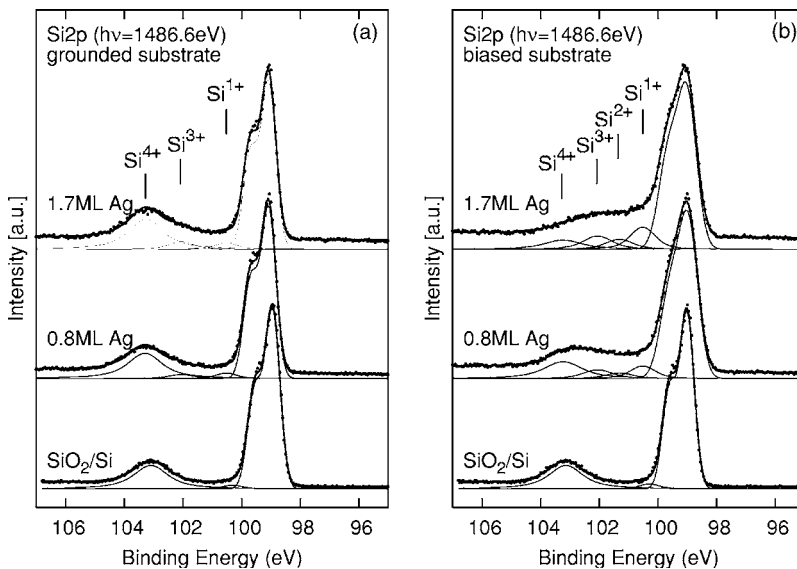


FIG. 3. The Si 2*p* core-level spectra for different Ag amounts deposited on grounded (left-hand side) and biased (right-hand side) substrate. Thin lines represent the chemically shifted components after core-line decomposition.

The deposition of silver on grounded and biased substrates shifts the silicon peak by 20 meV towards higher binding energy. The shift is caused by the downward band bending which accompanies the initial increase in conductance at the surface. The band-bending effect shifts all spectra in the same manner, so in order to make an easier comparison we aligned the lines after metal deposition with the initial silicon line. With an increase of metal deposition on grounded substrate [Fig. 3(a)], the silicon 4+ oxide line becomes broader and a second state displaced by 2.0 eV towards lower binding energy is formed. This feature is associated with the Si<sup>3+</sup> oxidation state of silicon<sup>19</sup> and its intensity increases slightly with increasing amount of deposited silver. Contrary to the grounded substrate, the deposition on biased substrate results in higher intensity from the Si<sup>1+</sup> state and appearance of the intermediate oxidation states Si<sup>2+</sup> and Si<sup>3+</sup> [Fig. 3(b)]. The deposition of 1.7 ML of silver leads to reduced intensity from the Si<sup>4+</sup> state with simultaneous increase of lower oxidation state contribution. The increase is accompanied by oxygen release from the oxide film and is related to the preferential sputtering of oxygen by the incident Ag ions.

Only a minor oxide reduction in the case of the grounded substrate could be explained by the distinctly lower sputtering yields for Si and O atoms in the present case. Calculations performed with the SRIM package<sup>20</sup> predict a sputtering yield value of 0.04 atom/ion for oxygen atoms and 0.0028 atom/ion for silicon whereas for the biased substrate the corresponding values are 0.65 and 0.12 atom/ion. It should be noted, however, that the sputtering yield changes under bombardment due to the surface roughness and damage, so the calculated values are not absolute but rather give a qualitative notion of the yield difference.

The Ag 3*d*<sub>5/2</sub> core-level lines of 0.8 ML silver deposited on the grounded substrate (upper curve) and on the biased substrate (lower curve) are presented in Fig. 4. Both spectra show pronounced shifts of 0.55 and 0.35 eV to larger binding energies for grounded and biased substrates, respectively. The shift is mainly due to the final-state effect in silver clusters caused by a delay in the relaxation time of the photohole as compared to the time of the photoelectron emission.<sup>21</sup> No

components related to silver oxide are detected. In addition to the binding-energy shift, the Ag core-level line of silver deposited onto grounded substrate shows an increase in the asymmetry and width of the peak. This change in line shape may be attributed to a broader size distribution of deposited clusters. Indeed, the final-state energy depends on cluster size since the cluster acts as a spherical capacitor and the final-state energy depends on  $e^2/2r$ .<sup>21</sup> Therefore, broadening of the core-level line implies the presence of a variety of cluster sizes on the substrate.

The latter is supported by the size distribution of Ag islands depicted in Fig. 5. The distributions were obtained by analyzing SEM images taken on samples with 7 ML of silver. It is seen that the growth of silver on grounded substrate (shown with open symbols) is characterized by broad size distribution of metal islands with a mean island size of

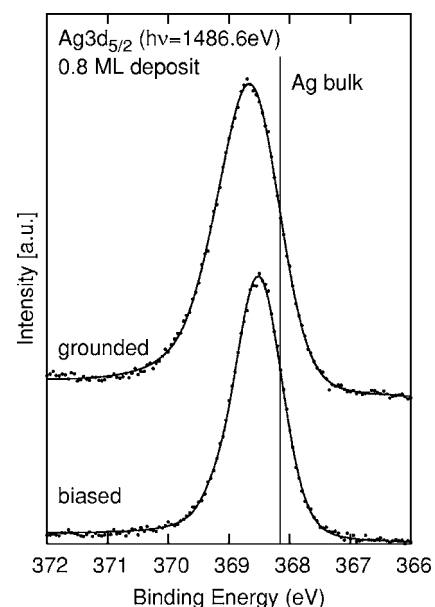


FIG. 4. The Ag 3*d*<sub>5/2</sub> core-level spectra of 0.8 ML silver deposited on grounded (upper curve) and biased (lower curve) silicon substrate covered with 2 nm native silicon dioxide. The dots represent the measured spectra and the lines are the fit function.



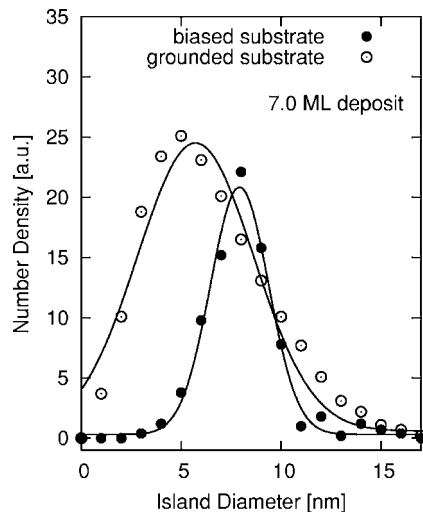


FIG. 5. Average island diameter of 7 ML silver deposited on grounded (open symbols) and biased (filled symbols) silicon substrate covered with 2 nm native silicon dioxide.

5.3 nm. The distribution for the biased substrate (shown with filled symbols) differs significantly from the case of grounded substrate and shows narrower dispersion and increased cluster size. Narrowing of the size distribution indicates more homogeneous nucleation of the film stimulated by the point defects on the oxide surface. Such surface defects are impact induced adatoms, adatom clusters, surface vacancies, and surface vacancy clusters originating from the ion bombardment of the surface. The observed island size increase in the case of the biased substrate is most likely due to an enhanced surface mobility of adatoms and crystallites leading to earlier film coalescence as previously discussed by Marinov.<sup>12</sup> On the other hand, there are other mechanisms influencing the formation of islands such as island fragmentation,<sup>22–24</sup> adatom sputtering,<sup>25</sup> and the presence of pinning centers.<sup>26</sup> The contribution of each separate mechanism on island formation kinetics remains to be determined.

The incident Ag ions may not only affect the nucleation process but also the film's growth mode. The procedure of using ion bombardment to change the growth mode from three dimensional to layer-by-layer growth was proposed by Rosenfeld *et al.*,<sup>14</sup> who used short argon ion pulses during the vapor phase deposition, namely, each time when the monolayer is completed. The ion pulse creates a high density of islands on the monolayer as it is completed, so there is a reduction in the average island size, while on top of the islands the nucleation probability stays low. In order to verify whether a similar mechanism may take place in our case, we measured the surface roughness of Ag films deposited on grounded and biased substrates at different coverages. The corresponding results of the surface roughness values measured with AFM are presented in Table I. It is evident that biasing the substrate leads to a significantly smooth film morphology compared to the grounded substrate which gives some support to the above proposed model. It is, however, difficult to assess its individual contribution to the film growth kinetics.

TABLE I. Surface roughness for different amounts of deposited silver as deduced from AFM measurements.

Silver coverage	$R_a$ (grounded substrate) (nm)	$R_a$ (biased substrate) (nm)
SiO <sub>2</sub> substrate	0.1	0.1
7.0 ML	0.73	0.31
14 ML	1.28	0.63
27 ML	1.60	0.81
54 ML	2.09	0.93

#### IV. CONCLUSIONS

We have presented an investigation of the interface formation between silver films prepared by pulsed arc deposition on silicon covered with a native silicon oxide layer. The evolution of the valence band and core-level spectra implies different growth kinetics of silver films deposited on grounded and biased substrates. Biasing the substrate increases the kinetic energy of incident silver ions, leading to an enhanced ion induced oxide reduction and accumulation of silicon on the surface. Compared to the grounded substrate, nucleation of silver is more homogeneous on the biased substrate, resulting in earlier coalescence of silver films and growth of smoother films. Furthermore, it is safe to assume that the effective formation of the transition layer may result in improved adhesion properties of silver films, thus making them compatible for use in many applications where adhesion plays a crucial role.

#### ACKNOWLEDGMENTS

The authors would like to thank Peter Reimann for fruitful discussions and Dr. Teresa de los Arcos for careful reading of the manuscript. Financial support of the Swiss Federal Office of Energy is gratefully acknowledged.

- <sup>1</sup>H. A. Macleod, *Thin Films Optical Filters* (Macmillan, New York, 1986).
- <sup>2</sup>A. K. Sarychev and V. M. Shalaev, *Phys. Rep.* **335**, 275 (2000).
- <sup>3</sup>D. J. Bergman and D. Stroud, *Solid State Phys.* **46**, 14 (1992).
- <sup>4</sup>V. M. Shalaev, *Phys. Rep.* **272**, 61 (1996).
- <sup>5</sup>G. Hass, J. B. Heaney, H. Herzig, J. F. Osantowski, and J. J. Triolo, *Appl. Opt.* **14**, 2639 (1975).
- <sup>6</sup>I. Dima, B. Popescu, F. Iova, and G. Popescu, *Thin Solid Films* **200**, 11 (1991).
- <sup>7</sup>G. Leftheriotis, S. Papaefthimiou, and P. Yianoulis, *Solid State Ionics* **136–137**, 655 (2000).
- <sup>8</sup>M. Arbab, *Thin Solid Films* **381**, 15 (2001).
- <sup>9</sup>Y. Tachibana, K. Kusunoki, T. Watanabe, K. Hashimoto, and H. Ohsaki, *Thin Solid Films* **442**, 212 (2003).
- <sup>10</sup>E. Masetti, J. Bulir, S. Gagliardi, V. Janicki, A. Krasilnikova, G. Di Santo, and C. Coluzza, *Thin Solid Films* **455–456**, 468 (2004).
- <sup>11</sup>J. Szczyrbowski, A. Dietrich, and K. Hartig, *Sol. Energy Mater.* **16**, 103 (1987).
- <sup>12</sup>M. Marinov, *Thin Solid Films* **46**, 267 (1977).
- <sup>13</sup>L. Pranevichus and S. Tamulevichus, *Nucl. Instrum. Methods Phys. Res.* **209**, 179 (1983).
- <sup>14</sup>G. Rosenfeld, R. Servaty, C. Teichert, B. Poelsema, and G. Comsa, *Phys. Rev. Lett.* **71**, 895 (1993).
- <sup>15</sup>J. M. Laferti, *Vacuum Arcs: Theory and Applications* (Wiley, New York, 1980).
- <sup>16</sup>M. G. Garnier, T. de los Arcos, J. Boudaden, and P. Oelhafen, *Surf. Sci.* **536**, 130 (2003).
- <sup>17</sup>S. Doniach and M. Sunjic, *J. Phys. C* **3**, 285 (1970).
- <sup>18</sup>D. A. Shirley, *Phys. Rev. B* **5**, 4709 (1972).

- <sup>19</sup>F. J. Himpsel, F. R. McFeely, A. Taleb-Ibrahimi, J. A. Yarmoff, and G. Hollinger, *Phys. Rev. B* **38**, 6084 (1988).
- <sup>20</sup>SRIM, Stopping and Range of Ions and Matter software is downloadable at <http://www.srim.org>
- <sup>21</sup>G. K. Wertheim, S. B. DiCenzo, and D. N. Buchanan, *Phys. Rev. B* **33**, 5384 (1986).
- <sup>22</sup>E. Chason and B. Kellerman, *Nucl. Instrum. Methods Phys. Res. B* **127/128**, 225 (1997).
- <sup>23</sup>J. Sillanpää and I. Koponen, *Nucl. Instrum. Methods Phys. Res. B* **142**, 67 (1998).
- <sup>24</sup>X. Zhou and H. Wadley, *Surf. Sci.* **487**, 159 (2001).
- <sup>25</sup>G. Carter, *Vacuum* **55**, 235 (1999).
- <sup>26</sup>B. Degroote, A. Vantomme, H. Pattyn, and K. Vanormelingen, *Phys. Rev. B* **65**, 195401 (2002).